Jpn. J. Appl. Phys. Vol. 34 (1995) pp. 2197-2206
Part 1, No. 5A, May 1995

Charge State Dependences of Positron Trapping Rates Associated with Divacancies and Vacancy-Phosphorus Pairs in Si

Atsuo KAWASUSO*, Masayuki HASEGAWA, Masashi SUEZAWA, Sadae YAMAGUCHI and Koji SUMINO
Institute for Materials Research, Tohoku University, Sendai 980, Japan

(Received January 26, 1995; accepted for publication March 18, 1995)

Charge state dependences of positron trapping rates associated with divacancies and vacancy-phosphorus pairs in Si have been studied by controlling the Fermi level systematically. The specific trapping rates of both a divacancy and a vacancy-phosphorus pair increase with an increase in the negative charge on them. A positively charged divacancy shows no detectable positron trapping. Such charge state dependences of the positron trapping rates clearly show that the long-range Coulomb interactions between a positron and a charged divacancy or a charged vacancy-phosphorus pair play an important role in the trapping process.

KEYWORDS: divacancy, vacancy-phosphorus pair, Si, positron lifetime, positron trapping, electron irradiation

1. Introduction

Divacancies are a dominant species of defects in a silicon (Si) crystal irradiated with fast particles at room temperature.[1,2] This is because monovacancies are too mobile to survive at such a temperature.[2,3] Both the atomic and electronic structures of a divacancy in Si have so far been investigated extensively by various experimental techniques, such as electron paramagnetic resonancen (ESR),[4] infrared absorption (IR),[5-9] photoconductivity (PC)[10,11] and deep level transient spectroscopy (DLTS).[12-18] It is now established that three energy levels are associated with a divacancy within the band gap at $E_c-0.23$ eV, $E_c-0.42$ eV and $E_V+0.27$ eV,[12] where E_C and E_V are the energies of the bottom of the conduction band and the top of the valence band, respectively. Thus, four different charge states (V_2^{2-}, V_2^-, V_2^0 and V_2^+) are available for a divacancy, depending on the Fermi level of the crystal. Vacancy-phosphorus (VP) pairs are also known to be one of the main defects introduced by irradiation in phosphorus-doped Si.[1,2] The properties of a VP pair have also been studied by various techniques.[19-22] Since a VP pair has one energy level within the band gap at $E_C-0.44$ eV, two different charge states (VP^- and VP^0) are available for a VP pair, depending on the Fermi level.

Positron lifetime measurement is a powerful technique for detecting vacancy-type defects in crystal.[23] Recently, this method has been extensively applied to the investigation of defects in semiconductors.[24,25] The positron lifetime is determined by an overlap integral between the positron and electron wave functions. Hence, the positron lifetime has the tendency to increase with the size of a vacancy cluster where a positron annihilates. On the other hand, the positron trapping rate of a defect reflects the interaction of the defect with a positron. In the case of metals, the Coulomb attraction between a positron and a vacancy is weakened due to the screening by free electrons. Since such a screening effect is reduced in semiconductors due to the low free-electron density, the long range Coulomb interaction is expected to act between a positron and a charged defect. Thus, the trapping rate of a defect is expected to depend on the charge state of the defect. The trapping rate obtained from a positron lifetime measurement is proportional to the specific trapping rate and the defect concentration. In order to clarify the interaction between a positron and a defect, it is important to determine the absolute value of the specific trapping rate. This is, however, a difficult task since the defect concentration must be known. In addition, the charge state of the defect should also be specified in the case of semiconductors.

Some reports have already been published on the specific trapping rates of divacancies and VP pairs.[26-29] However, the concentrations and charge states of the defects seems to be inadequately estimated in most works. Here, we attempted to determine the specific trapping rate of divacancies and VP pairs from positron lifetime measurements according to their dependence on their charge states. The concentrations of divacancies and VP pairs were determined from Hall effect measurements prior to the positron lifetime measurement. The charge states of divacancies and VP pairs were controlled by shifting the Fermi level of the crystal by changing the dopant species, their concentrations and the irradiation fluence.

2. Experimental

Specimens used in the experiment were prepared from Si crystals grown by the floating-zone method. The crystals are classified into two groups, Si:P (n-type) and Si:B (p-type) which are doped with phosphorus and boron, respectively. Defects were generated by irradiating crystal blocks with various fluences of 15 MeV electrons at room temperature. The blocks were kept at room temperature during irradiation with running water. Specimens were cut from the irradiated blocks and polished chemically with CP4 reagent. The specimen was finished into a size of about $5\times5\times0.8$ mm^3 and $6\times5\times0.8$ mm^3 for the measurements of Hall effect and positron lifetime, respectively. Table I shows the dopant species, their concentrations and the

*Present address: JAERI, Takasaki Radiation Chemistry Research Establishment Institute, Watanuki-machi 1233, Takasaki, Gunma 370-12, Japan.

Table I. Species and concentrations of dopants and irradiation fluence of specimen.

Specimen	Dopant (cm^{-3})	Fluence (e^-/cm^2)
Si:P-1	P: 1.7×10^{16}	1.5×10^{16}
-2		1.0×10^{17}
-3		1.5×10^{17}
-4		2.0×10^{17}
-5		3.0×10^{17}
-6		5.0×10^{17}
-7		8.0×10^{17}
Si:B-1	B: 1.0×10^{16}	1.5×10^{16}
-2		3.0×10^{16}
-3		1.0×10^{17}
-4		1.5×10^{17}
-5		2.0×10^{17}
-6		3.0×10^{17}
-7		5.0×10^{17}
-8		8.0×10^{17}

irradiation fluence.

Hall effect measurements were performed by means of the van der Pauw method[30] between 90 K and room temperature to determine the Fermi levels of crystals and the concentrations of defects. The Hall coefficient R_H (cm^3) was related to the electron density, n (cm^{-3}), or the hole density, p (cm^{-3}),

$$n, p=\frac{1}{e\cdot R_H}, \tag{1}$$

where e is the elementary electronic charge (1.602×10^{-19} C).

$^{22}NaCl$ ($\sim4\times10^5$ Bq) was deposited onto a Mylar thin film with a thickness of ~5 μm as a positron source. It was sandwiched by two specimens and positron lifetime measurements were carried out at room temperature using a conventional spectrometer with a time resolution of $\sim$200 ps. The total counts of 2×10^6 were accumulated for each spectrum. The source component was $\sim$350 ps with the intensity of $\sim$10%. After subtracting the source and background components, the lifetime spectrum was resolved into two or three lifetime components using a fitting program of PATFIT-88.[31] For example, in the case of three-component analysis, the spectrum was fitted by the relation

$$L(t)=(I_1/\tau_1)\exp(-t/\tau_1)+(I_2/\tau_2)\exp(-t/\tau_2)+(I_3/\tau_3)\exp(-t/\tau_3). \tag{2}$$

Here, τ_i ($i=1$, 2, 3) are the positron lifetimes and I_i are the intensities ($I_1+I_2+I_3=1$). In the case that the trapping mode[23] is valid as a good approximation, the lifetimes are given by

$$\tau_1=\frac{1}{1/\tau_B+\kappa_{D1}+\kappa_{D2}}, \tag{3}$$

$$\tau_2=\tau_{D1}, \tag{4}$$

$$\tau_3=\tau_{D2}, \tag{5}$$

where τ_B is the positron lifetime in the bulk, which was determined to be 222 ± 2 ps from the measurement of unirradiated Si, and τ_{D1} and τ_{D2} are the positron lifetimes at different defects denoted by $D1$ and $D2$. κ_{D1} and κ_{D2} are the trapping rates of defects $D1$ and $D2$, respectively. They are given by

$$\kappa_{D1}=\frac{I_2}{I_1}\{1/\tau_B-(1-I_3)/\tau_{D1}-I_3/\tau_{D2}\}, \tag{6}$$

$$\kappa_{D2}=\frac{I_3}{I_1}\{1/\tau_B-I_2/\tau_{D1}-(1-I_2)/\tau_{D2}\}. \tag{7}$$

Equation (3) indicates that if the trapping model is valid the lifetime τ_1 should coincide with the right-hand side calculated from eqs. (4) through (7). This criterion is used to check the validity of the trapping model. In the two-component analysis, we neglect τ_3, I_3 and κ_{D2} in the above equations.

The trapping rate is given by

$$\kappa=\mu\cdot C=\nu_+\cdot\sigma\cdot C, \tag{8}$$

where C is the defect concentration, μ is the specific trapping rate, ν_+ is the thermal velocity of a positron ($\sim10^7(T/300)^{1/2}$ cm/s, where T denotes the temperature) and σ is the trapping cross section. Thus, we can determine the values of specific trapping rate and cross section if the defect concentration is known.

3. Results and Discussion

We first report the results of Hall effect measurements and determine the Fermi levels of specimens and the concentrations of divacancies and *VP* pairs. Subsequently, we will report the results of positron lifetime measurements and determine the specific trapping rates for various charge states of divacancies and *VP* pairs.

3.1 *Fermi level and defect concentration*

Figures 1 and 2 show the temperature dependences of carrier densities for Si:P and Si:B specimens, respectively, obtained from Hall coefficients using eq. (1). It is found that the carrier densities are reduced by irradiation, and the specimen becomes semi-insulating at a high fluence in both n- and p-type specimens. This is because divacancies and *VP* pairs induced by irradiation act as acceptors in the n-type crystal (Si:P), and divacancies act as donors in the p-type crystal (Si:B), as discussed below.

We now show how the Fermi level E_F changes with the fluence. E_F is related to the electron or hole density, n or p, by

$$n=2\left(\frac{2\pi m_e kT}{h^2}\right)^{3/2}\exp\left(\frac{E_F-E_C}{kT}\right), \tag{9}$$

$$p=2\left(\frac{2\pi m_h kT}{h^2}\right)^{3/2}\exp\left(\frac{E_V-E_F}{kT}\right), \tag{10}$$

where m_e and m_h are the effective masses of an electron and a hole, respectively, and the pre-exponential factors are the effective densities of states of the conduction band and the valence band.

Figure 3(a) shows how the Fermi levels shift with the fluence in Si:P and Si:B specimens estimated from eqs. (9) and (10). The Fermi level approaches the middle of the band gap with increaseing fluence, irrespective of

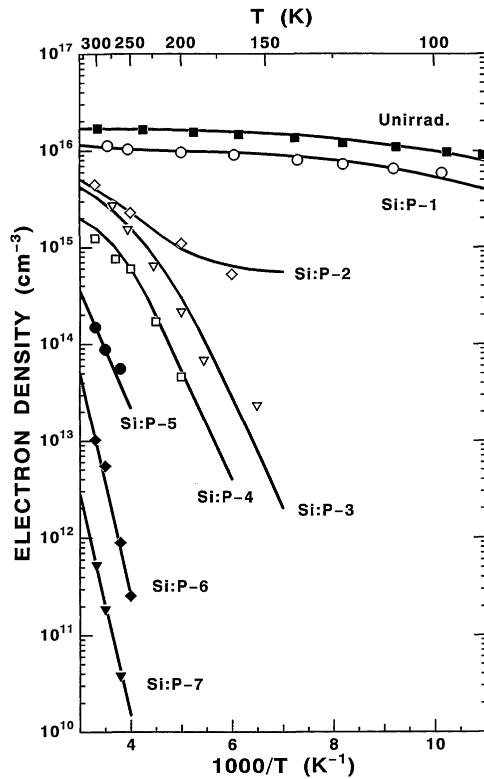

Fig. 1. Free-electron density as a function of the inverse of temperature for various Si:P specimens.

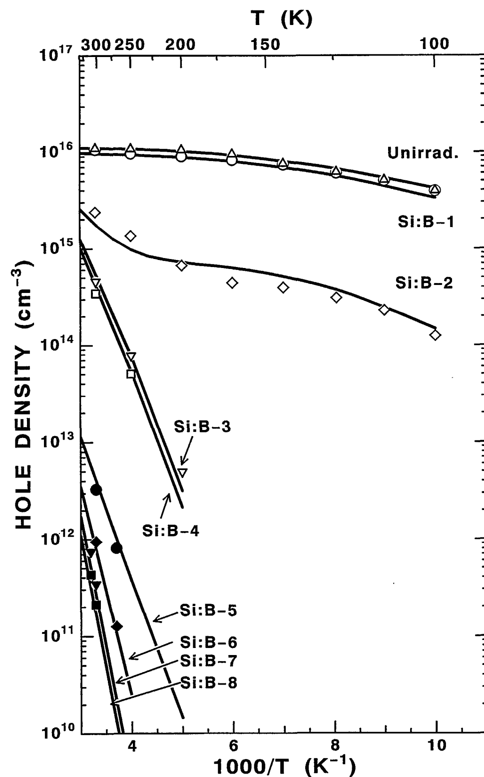

Fig. 2. Free-hole density as a function of the inverse of temperature for various Si:B specimens.

the conduction type of the crystal. This shows that the irradiation-induced defects act as acceptors in Si:P specimens and as donors in Si:B specimens, namely,

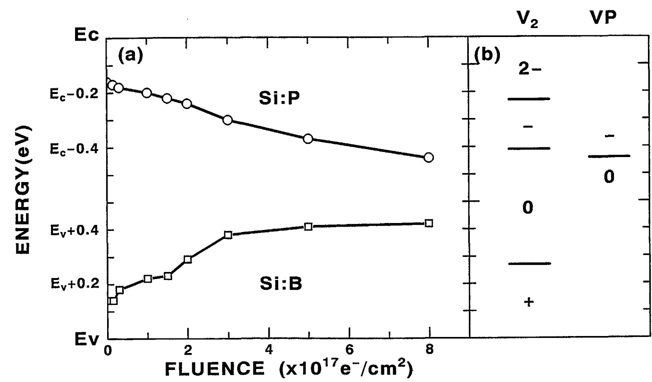

Fig. 3. (a) Fermi levels in Si:P specimens (open circles) and Si:B specimens (open squares) plotted against the fluence. (b) Energy levels and charge states of a divacancy and a *VP* pair.

they are of "amphoteric nature". The decrease of Fermi level with increasing fluence is gradual around $E_C-0.23$ eV in Si:P specimens. This suggests the defects have acceptor levels there,[33] which is close to the second acceptor level of a divacancy shown in Fig. 3(b). Thus, it is suggested that divacancies are introduced by irradiation. With further increase in the irradiation fluence, the Fermi level approaches $E_C-0.44$ eV which is close to the acceptor level of a *VP* pair. Thus, *VP* pairs are also suggested to be introduced by irradiation. On the other hand, the increase of Fermi level in the Si:B specimen is first gradual around $E_V+0.25$ eV. This may be attributed to the donor level of a divacancy. With further increase in the fluence, the Fermi level approaches to the middle of the band gap. This behavior cannot be interpreted in terms of the energy scheme of a divacancy since a divacancy has no donor level at the middle of the band gap. Thus, another donor level at the middle of the band gap which is related to irradiation-induced defects should be taken into account. According to the DLTS study by Ono and Sumino,[33] hole traps at $E_V+0.53$ eV are introduced by 15 MeV electron irradiation. Our result can therefore be explained by the idea that such defects are introduced in Si:B specimens, which act as donors.

Thus, we propose that divacancies and *VP* pairs were introduced by irradiation. The existence of divacancies has also been confirmed from IR measurements.[34] A divacancy acts as an amphoteric defect to compensate free electrons or free holes in n-type or p-type Si. A *VP* pair is not an amphoteric defect since it has only one acceptor level. The above results show that the Fermi level is controlled to be deep by high irradiation fluences. This means that the charge state of a divacancy changes in the order of $V_2^{2-} \rightarrow V_2^{-} \rightarrow V_2^{0}$ and $V_2^{+} \rightarrow V_2^{0}$ in the Si:P and Si:B specimens, respectively, with the increase in fluence. Similarly, the charge state of a *VP* pair changes in the order of $VP^{-} \rightarrow VP^{0}$ in the Si:P specimen.

Next, we undertake to reproduce the temperature dependences of free-carrier densities shown in Figs. 1 and 2 using the occupation statistics of divacancies and *VP*

pairs to confirm that these two types of defects are dominant in irradiated Si crystals.

The neutrality condition of a crystal is generally given by

$$n+N_{\rm SA}^{-}+\sum_{i}N_{{\rm A}_i}^{-}=p+N_{\rm SD}^{+}+\sum_{j}N_{{\rm D}_j}^{+}, \tag{11}$$

where $N_{\rm SA}^{-}$ and $N_{\rm SD}^{+}$ are the concentrations of ionized shallow acceptors and shallow donors, respectively, and $N_{{\rm A}_i}^{-}$ and $N_{{\rm D}_j}^{+}$ are the concentrations of ionized i-th kind of acceptors and j-th kind of donors, respectively, all of which are introduced by irradiation. The concentration of the ionized donors $N_{\rm D}^{+}$ ($N_{\rm SD}^{+}$ or $N_{{\rm D}_j}^{+}$) and that of the ionized acceptors $N_{\rm A}^{-}$ ($N_{\rm SA}^{-}$ or $N_{{\rm A}_i}^{-}$) are given by

$$N_{\rm D}^{+}=\frac{N_{\rm D}}{1+g_{\rm D}\exp\left(\dfrac{E_{\rm F}-E_{\rm D}}{kT}\right)}, \tag{12}$$

$$N_{\rm A}^{-}=\frac{N_{\rm A}}{1+g_{\rm A}\exp\left(\dfrac{E_{\rm A}-E_{\rm F}}{kT}\right)}, \tag{13}$$

respectively, where $N_{\rm D}$ and $N_{\rm A}$ are the concentrations of the donors and acceptors, respectively, and $E_{\rm D}$ and $E_{\rm A}$ are their energy levels, and $g_{\rm D}$ and $g_{\rm A}$ are their degeneracy factors. The value of the degeneracy factor depends on the electronic structure of the defect. For shallow donors and acceptors, $g_{\rm D}=2$ and $g_{\rm A}=1/2$, respectively. For the defects, $g_{\rm D}=g_{\rm A}=2$ if they are initially empty or occupied by paired electrons. Alternatively, $g_{\rm D}=g_{\rm A}=1/2$ if they are initially occupied by the unpaired electrons, and are finally empty or occupied by paired electrons.[35] Substituting eqs. (9), (10), (12) and (13) into eq. (11) yields a nonlinear equation with respect to $E_{\rm F}$. If the concentrations and energy levels of donors and acceptors are given, $E_{\rm F}$ can be calculated by solving the nonlinear equation, and n and p can be estimated from eqs. (9) and (10). The obtained n and p should coincide with those determined experimentally if given concentrations and energy levels of donors and acceptors are correct. Thus, we can determine the concentrations of donors and acceptors by treating them as fitting parameters.

The nonlinear equation was solved numerically using a computer program developed by Kamiyama.[36] In the calculation, the acceptor levels of divacancies and *VP* pairs were adopted for $E_{\rm A}$ in Si:P specimens and the donor levels of divacancies and $E_{\rm V}+0.53$ eV for $E_{\rm D}$ in Si:B specimens, as mentioned above. The solid lines in Figs. 1 and 2 show the results of the calculation. It is seen that the temperature dependences of carrier densities are reproduced in a satisfactory manner.

Figure 4 shows the concentrations of divacancies and *VP* pairs as a function of fluence. The concentration of the donor levels at $E_{\rm V}+0.53$ eV in Si:B specimens is ~1/5 that of divacancies. The latter defects will not be discussed hereafter since they are not related to positron trapping centers. The concentration of *VP* pairs increases slowly with increasing fluence and tends to saturate. On the other hand, the concentration of divacancies in Si:B specimens increases linearly with

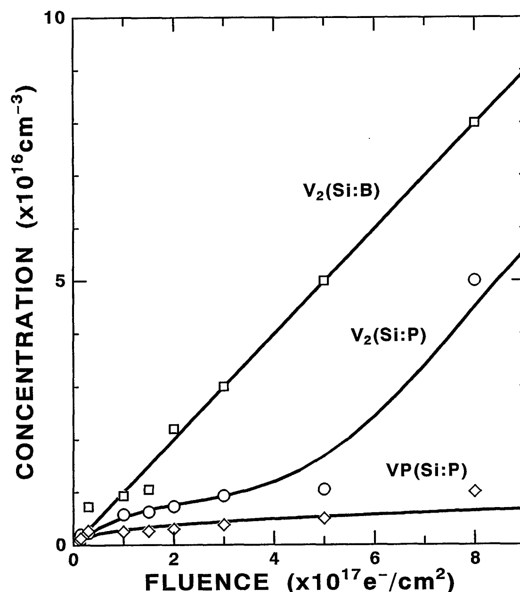

Fig. 4. Concentrations of divacancies and *VP* pairs as a function of fluence. Open squares and open circles show the concentrations of divacancies in Si:B and Si:P specimens, respectively. Open diamonds show the concentration of *VP* pairs in Si:P specimens.

fluence. The production rate of divacancy is estimated to be ~0.1 cm^{-1} which is higher than the production rate of divacancies, ~0.03 cm^{-1}, in primary collision.[1] These indicate that divacancies are produced not only by primary collision but also by means of the pairing of monovacancies. The concentration of divacancies in Si:P specimens shows different behavior from that in Si:B specimens; the production rate of divacancies is rather low in the low fluence range, but increases rapidly in the high fluence range. Thus, we show that the fluence dependence of divacancy concentration depends on the conduction type of specimens. A similar result was reported by Svensson and colleagues[15,17] for tin-doped Si. They showed that the production rate of divacancies in tin-doped Si was suppressed in comparison with undoped Si. They attributed such a reduction in the production rate of divacancies to the trapping of monovacancies by tin atoms. However, they ruled out another possibility that single interstitials recombine with divacancies. Considering the fact that *VP* pairs are also produced in Si:P specimens, the low production rate of divacancies in this type of specimen may be interpreted to be a result of the fact that phosphorus atoms work as effective trapping centers for mobile monovacancies. However, it does not fully explain the process since the difference in the concentrations of divacancies in two types of specimens is not equal to half the concentration of *VP* pairs ($[V_2]_{\rm Si:B}-[V_2]_{\rm Si:P}\neq[VP]_{\rm Si:P}/2$). It is probable that the reduction of the production rate of divacancies is also caused by the recombination between divacancies and single interstitials. The high production rate of divacancies in the high fluence range in Si:P specimens may be interpreted in terms of the idea that the trapping of monovacancies by phosphorus atoms and the recombination of divacancies and single interstitials are reduced there.

In order to confirm the validity of such an idea, we performed a model simulation for the formation processes of defects under irradiation using chemical rate equations given by Damask and Dienes.[37] Here, we give only the essence of the results. (For detailed discussions, see appendix.) In the simulation, it is shown that the formation process of divacancies is affected by phosphorus atoms. In phosphorus-free (undoped) Si the concentrations of monovacancies and single interstitials introduced by irradiation approach stationary values in the initial stage of irradiation. As a result, the concentration of divacancies increases linearly with fluence. This situation corresponds to the case of Si:B specimens.[38] On the other hand, in phosphorus doped Si, monovacancies are trapped by phosphorus atoms to yield excess interstitials which do not recombine with monovacancies. As a result, the excess interstitials recombine with divacancies and reduce the concentration of the latter. This is the explanation for the low production rate of divacancies in the low fluence range. The concentration of *VP* pairs approaches a saturated value with prolonged irradiation. Then, monovacancies are no longer trapped by phosphorus atoms and recombine only with interstitials. As a result, the concentration of divacancies increases at the same rate as in undoped Si.

3.2 *Positron lifetime*

First, the results for Si:B specimens are reported. This type of specimen contains predominantly divacancies after irradiation. We thus decomposed the lifetime spectra into two lifetime components (those related to bulk and to divacancies). Figure 5 shows the lifetimes τ_1 and τ_2 and intensity I_2 as a function of the fluence. The magnitude of lifetime τ_1 (bulk) agrees well with that expected from the trapping model. This assures the validity of analysis based on the trapping model. The lifetime τ_2 (defect) is about 295 ps and is nearly independent of the irradiation fluence. This shows that the species of positron trapping centers does not change with the fluence. The lifetime 295 ps is longer than the lifetime at a monovacancy (~250 ps).[39] Accordingly, this lifetime component is assumed to be related to divacanies. In fact, it was found that the annealing behavior of the 295 ps component well agrees with that of divacancies observed by IR measurement.[40] Moreover, the lifetime of 295 ps is comparable to the lifetime at a divacancy reported by Kwete *et al.*[28,41]

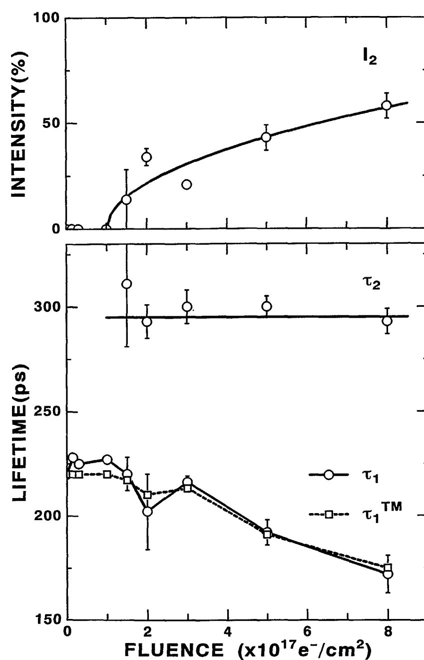

Fig. 5. Positron lifetimes (τ_1 and τ_2) and intensity (I_2) as a function of the fluence for Si:B specimens. τ_1^{TM} denotes the first lifetime expected from the trapping model (see text).

The trapping rate for the second lifetime component has been estimated from the intensity shown in Fig. 5 using eq. (6). Figure 6 shows the fluence dependence of the trapping rate for the second lifetime component. The trapping rate is lower than the detection limit in the fluence range below 1×10^{17} e$^-$/cm^2, but increases linearly with the fluence in the higher fluence range. Most divacancies are in the positive charge state in the fluence range below 1×10^{17} e$^-$/cm^2 as shown in Fig. 3. This may suggest that the trapping rate of a positively charged divacancy is too low to be detected. This seems to be due to the Coulomb repulsion between a positron and a positively charged divacancy, as discussed later. The increase of the trapping rate above the fluence of 1×10^{17} e$^-$/cm^2 is explained as being due to the transformation of the charge state of divacancies from positive to neutral due to the shift of Fermi level and trapping of a positron by a neutral divacancy. The linear increase of the trapping rate indicates that the concentration of divacancies is proportional to the fluence. This scenario agrees with the result shown in Fig. 4. It is now possible to estimate the specific trapping rate for neutral and positive divacancies from the trapping rate and the concentration of divacancies. This will be discussed later.

Next, the results on Si:P specimens are reported. As shown in §3.1, this specimen contains mainly divacancies and *VP* pairs. It is shown that these two kinds of defects act as positron trapping centers in phosphorus-doped Si.[42] However, three-component analysis (bulk,

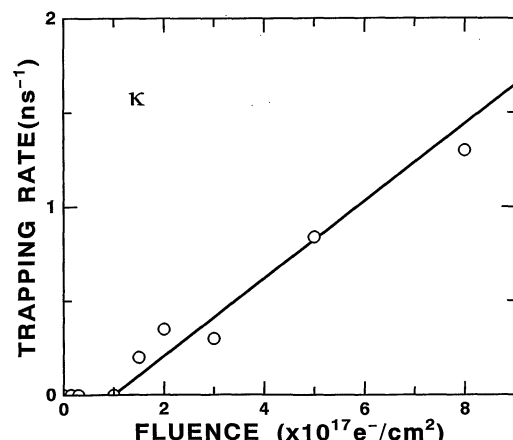

Fig. 6. Positron trapping rate (κ) related to the second lifetime component in Fig. 5 as a function of the fluence.

VP pairs and divacancies) of the lifetime spectrum using free parameters yield no meaningful results due to large statistic error in most cases. We therefore perform three-component analysis by fixing one of the lifetimes. Since reliable data on the lifetime at *VP* pairs have already been reported by Mäkinen and coworkers,[29,39] we adopt their values here. Their works show that the positron lifetimes at the singly negative and neutral *VP* pairs are ~250 ps and ~265 ps, respectively. Such values are also supported by a theoretical work.[43] Since the singly negative *VP* pairs are dominant in the fluence range below 3×10^{17} e^-/cm^2, the lifetime at a *VP* pair may be fixed at 250 ps. Some *VP* pairs are in the neutral charge state at fluences of 5 and 8×10^{17} e^-/cm^2. Hence, the lifetime at a *VP* pais may shift slightly toward 265 ps. We thus examined to analyze the data by changing the lifetime from 250 ps to 265 ps for these fluences. However, the result of the analysis is not affected by such a small change of lifetime within statistical error. We therefore fix the lifetime at a *VP* pair to be 250 ps for these fluences as well.

Figure 7 shows the lifetimes τ_1 and τ_3 and intensities I_2 and I_3 for Si:P specimens as a function of the fluence obtained from the three-component analysis. The second lifetime was fixed to 250 ps for *VP* pairs. The first and third lifetime components were chosen to be free parameters. The lifetime τ_1 (bulk) agrees with that expected from the trapping model. This assures the validity of the analysis based on the trapping model. The lifetime τ_3 is ~320 ps in a low fluence range, but gradually decreases toward ~300 ps with increasing fluence. As reported in a previous work,[45] the lifetimes at a doubly negatively charged, a singly negatively charged and a neutral divacancy are 323, 310 and 295 ps, respectively, at room temperature. Since the charge state of divacancy changes from doubly negative to neutral with fluence, the fluence dependence of the lifetime τ_3 seems to reflect the charge state dependence of lifetime at a divacancy.

We estimated the trapping rates for the second and third lifetime components from the intensities shown in Fig. 7. Figure 8 shows the fluence dependences of the trapping rates, κ_2 and κ_3, which correspond to the second and third lifetime components, respectively. They show somewhat unusual behaviors. The trapping rate κ_2 first increases with the fluence and then decreases gradually to approach a constant. The trapping rate κ_3 first increases rapidly, decreases slightly and then increases again with fluence. These nonlinear fluence dependences of trapping rates are thought to reflect (i) nonlinear fluence dependence of the concentrations of divacancies and *VP* pairs shown previously and (ii) the charge-state-dependent specific trapping rates associated with divacancies and *VP* pairs. Solid lines in Fig. 8 show the fluence dependences of trapping rates obtained from the concentrations of divacancies and *VP* pairs shown in Fig. 4 and their specific trapping rates which will be derived in the following section. The rapid increase of the trapping rate κ_3 in the low fluence range is probably related to the fact that most divacancies are charged doubly negative, with which the specific trapping rate may be the highest. The slight decrease of κ_3 in the middle fluence range is explained by the transformation of the charge state of divacancies to singly negative and the low production rate of divacancies. The increase of κ_3 in the high fluence range may be due to the high production rate of divacancies. The fluence dependence of κ_2 can also be explained in a similar manner.

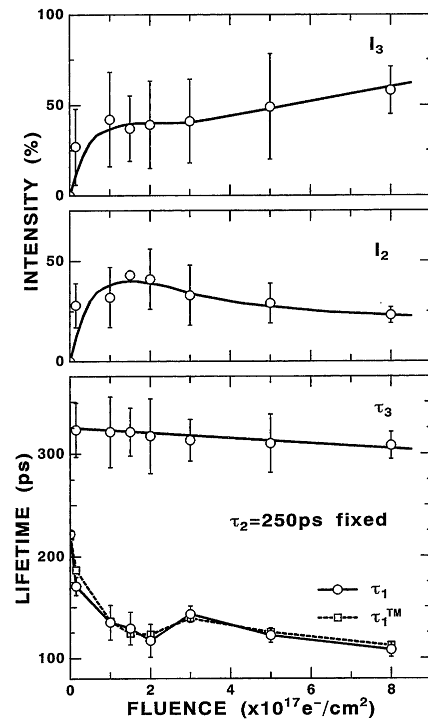

Fig. 7. Positron lifetimes (τ_1, τ_2 and τ_3) and intensities (I_2 and I_3) as a function of the fluence for Si:P specimens. The second lifetime component (τ_2) was fixed at 250 ps (see text). τ_1^{TM} is the same as in Fig. 5.

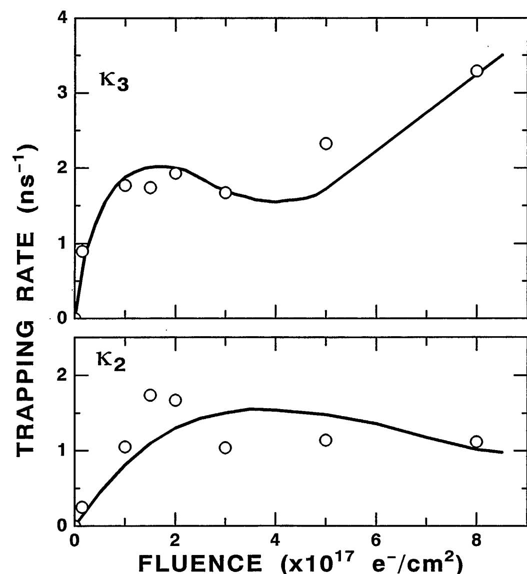

Fig. 8. Positron trapping rates (κ_2 and κ_3) related to the second and third lifetime components in Fig. 7 as a function of the fluence for Si:P specimens.

3.3 *Specific trapping rate*

Now we calculate the specific trapping rates of a divacancy and *VP* pair. Since both a divacancy and a *VP* pair can have different charge states ($V_2^{2-}, \cdots, V_2^+$, VP^- and VP^0), eq. (8) is extended as

$$\kappa = C_{V_2}(f_{V_2^{2-}}\mu_{V_2^{2-}} + f_{V_2^-}\mu_{V_2^-} + f_{V_2^0}\mu_{V_2^0} + f_{V_2^+}\mu_{V_2^+}), \quad (14)$$

$$\kappa = C_{VP}(f_{VP^-}\mu_{VP^-} + f_{VP^0}\mu_{VP^0}) \quad (15)$$

for divacancies and *VP* pairs, respectively, where μ_i and f_i are the specific trapping rate and the fraction of a defect i, respectively:

$$f_{V_2^{2-}} + f_{V_2^-} + f_{V_2^0} + f_{V_2^+} = 1, \quad (16)$$

$$f_{VP^-} + f_{VP_0} = 1. \quad (17)$$

The value of f_i is determined from the Fermi-Dirac distribution (eqs. (12) and (13)) and is shown in Table II.

Equations (14) and (15) are modified into more convenient forms. For *VP* pairs, eq. (15) is rewritten as

$$\kappa/C_{VP} = (\mu_{VP^-} - \mu_{VP^0}) f_{VP^-} + \mu_{VP^0}, \quad (18)$$

using eq. (17). In the case of Si:P specimens, $f_{V_2^0}$ and $f_{V_2^+}$ are negligible in the fluence range below 3×10^{17} e$^-$/cm^2 since most divacancies are charged to be doubly and singly negative. Thus, eq. (14) may be rewritten as

$$\kappa/C_{V_2} = (\mu_{V_2^{2-}} - \mu_{V_2^-}) f_{V_2^{2-}} + \mu_{V_2^-}. \quad (19)$$

In a similar way, since $f_{V_2^{2-}}$ and $f_{V_2^+}$ are negligible in the fluence range above 3×10^{17} e$^-$/cm^2, eq. (14) is rewritten as

$$\kappa/C_{V_2} = (\mu_{V_2^-} - \mu_{V_2^0}) f_{V_2^-} + \mu_{V_2^0}. \quad (20)$$

In the case of Si:B specimens, $f_{V_2^{2-}}$ and $f_{V_2^-}$ are negligible. Thus, eq. (14) is rewritten as

$$\kappa/C_{V_2} = (\mu_{V_2^0} - \mu_{V_2^+}) f_{V_2^0} + \mu_{V_2^+}. \quad (21)$$

Now we have κ/C for the defects as a function of f_i for a dominant charge state. Hence, the values of $\mu_{V_2^{2-}}, \cdots, \mu_{V_2^+}$, μ_{VP^-} and μ_{VP^0} are determined from the plot of κ/C against f_i. For example, the values of $\mu_{V_2^{2-}}$ and $\mu_{V_2^-}$ are determined from the plot of κ/C_{V_2} against $f_{V_2^{2-}}$, as seen from eq. (19). Figure 9 shows the plots of κ/C against f_i for the above four cases. The values of μ_i determined from these plots are summarized in Table III together with those determined by other authors. The specific trapping rate of a positively charged divacancy is lower than the detection limit ($<10^{14}$ s^{-1}). The specific trapping rate of a singly negatively charged divacancy is about an order of magnitude larger than that of a neutral divacancy. That of a doubly negatively charged divacancy is 3 times as large as that of a singly negatively charged divacancy. The specific trapping rate of a negatively charged *VP* pair is larger than that of a neutral *VP* pair by more than one order of magnitude. The specific trapping rate of a neutral divacancy agrees with those previously reported in its order of magnitude. However, those of negatively charged divacancies and the *VP* pair are 5 to 10 times larger than those reported by Mascher *et al.*[26] and Mäkinen *et al.*[29] These discrepancies are probably related to inaccuracies in the concentrations and charge states of the defects in their work.

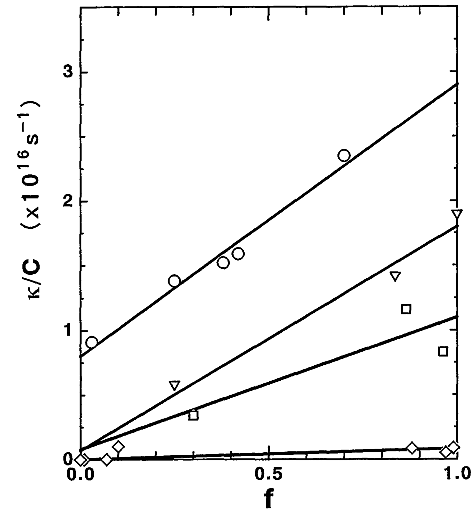

Fig. 9. The plot of κ/C against f_i: open circles, open squares, open diamonds are for doubly negatively, singly negatively, and neutral divacancies, respectively, and open triangles are for negatively charged *VP* pairs.

The above charge state dependence of specific trapping rates clearly shows that long-range Coulomb interaction acts between a positron and a charged defect. The undetectably small specific trapping rate of a positively charged divacancy may be interpreted in terms of the Coulomb repulsion between a positively charged

Table II. Fraction f_i of divacancies and *VP* pairs in various charge states.

Specimen	Fluence (e$^-$/cm^2)	$f_{V_2^{2-}}$	$f_{V_2^-}$	$f_{V_2^0}$	$f_{V_2^+}$	f_{VP^-}	f_{VP^0}
Si:P-1	1.5×10^{16}	0.70	0.30	0.00	0.00	1.00	0.00
-2	1.0×10^{17}	0.42	0.58	0.00	0.00	1.00	0.00
-3	1.5×10^{17}	0.38	0.62	0.00	0.00	1.00	0.00
-4	2.0×10^{17}	0.25	0.75	0.00	0.00	1.00	0.00
-5	3.0×10^{17}	0.03	0.96	0.01	0.00	0.99	0.01
-6	5.0×10^{17}	0.00	0.86	0.14	0.00	0.84	0.16
-7	8.0×10^{17}	0.00	0.30	0.70	0.00	0.25	0.75
Si:B-1	1.5×10^{16}	0.00	0.00	0.00	1.00	···	···
-2	3.0×10^{16}	0.00	0.00	0.01	0.99	···	···
-3	1.0×10^{17}	0.00	0.00	0.07	0.93	···	···
-4	1.5×10^{17}	0.00	0.00	0.10	0.90	···	···
-5	2.0×10^{17}	0.00	0.00	0.88	0.12	···	···
-6	3.0×10^{17}	0.00	0.00	0.97	0.03	···	···
-7	5.0×10^{17}	0.00	0.00	0.99	0.01	···	···
-8	8.0×10^{17}	0.00	0.00	0.99	0.01	···	···

Table III. Specific trapping rates of divacancies and *VP* pairs in various charge states (units: s^{-1}).

	Present	Mascher *et al.*[26]	Shimotomai *et al.*[27]	Kwete *et al.*[28]	Mäkinen *et al.*[29]
$\mu_{V_2^{2-}}$	2.9×10^{16}	3.7–7.4$\times10^{15}$	···	···	···
$\mu_{V_2^-}$	1.0×10^{16}	1.9–3.7$\times10^{15}$	···	···	···
$\mu_{V_2^0}$	8.1×10^{14}	0.5–1.0$\times10^{15}$	3.0×10^{14}	5.5×10^{14}	···
$\mu_{V_2^+}$	$<10^{14}$	···	···	···	···
μ_{VP^-}	1.8×10^{16}	···	···	···	2×10^{15}
μ_{VP^0}	6.8×10^{14}	···	···	···	···

divacancy and a positron. The large specific trapping rates of a negatively charged divacancy and *VP* pair show that the long-range Coulomb attraction acts between a positron and them. The trapping cross sections for doubly negatively charged, singly negatively charged and neutral divacancies are estimated to be $\sim 5.6\times 10^{-14}$ cm^2, $\sim 1.9\times 10^{-14}$ cm^2 and $\sim 1.6\times 10^{-15}$ cm^2, respectively, from eq. (8). If we simply assume that the trapping cross section is given by πr^2 with the effective trapping radius r, the trapping radii for doubly negatively charged, singly negatively charged and neutral divacancies are estimated to be $\sim$13 Å, $\sim$8 Å and $\sim$2 Å, respectively. It is interesting to note that the trapping radius of a neutral divacancy is comparable to the geometrical size of a divacancy. The differences in trapping radii of doubly negatively and singly negatively charged divacancies from that of a neutral divacancy are 11 Å and 6 Å, respectively. The former is about twice of the latter. This probably reflects the ratio of their charges.

We conclude that Coulomb attraction between a positron and a negatively charged divacancy or a *VP* pair enhances the specific trapping rate. A positron and a negatively charged defect have a long range attraction. The wave function of a positron trapped by the Coulomb potential may fairly extend. The situation is analogous to that of shallow donors and acceptors in semiconductors. However, the positron will ultimately be trapped in the deep ground state where the positron is localized in the vicinity of the vacant sites. Results of a theoretical study[46] indicate that positron trapping by a negatively charged vacancy occurs via two steps: a positron is at first trapped by one of the shallow "Rydberg" states originating from the Coulomb attraction, and then is successively transferred to the deep ground state. Namely, the Coulomb attraction provides a precursor state for positron trapping into the ground state. It will be interesting to clarify the details of such a trapping mechanism. It will be necessary to study, for example, the temperature dependence of the trapping rate of each charge state of divacancies and *VP* pairs. Such work will be reported elsewhere.

4. Conclusions

The specific trapping rates of various charge states of divacancies and *VP* pairs at room temperature were determined by controlling the Fermi level systematically. It is found that the specific trapping rate is sensitive to their charge state; the specific trapping rates of a negatively charged divacancy and a *VP* pair are much larger than those in the neutral charge states, and that of a positively charged divacancy is too low to be detected. These clearly indicate that the long-range Coulomb attraction acts between a positron and a negatively charged divacancy or a *VP* pair, while Coulomb repulsion acts between a positron and a positively charged divacancy.

Acknowledgments

We thank Dr. K. Masumoto and the technical staff at the Nuclear Science Institute, Tohoku University, for their help in electron irradiation.

Appendix

In order to explain the fluence dependence of the concentrations of divacancies and *VP* pairs shown in Fig. 4, we performed a simulation based on the chemical kinetics. Since divacancies and *VP* pairs are introduced in the phosphorus-doped Si, we consider the following reactions:

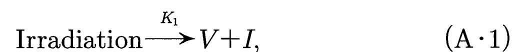

$$\text{Irradiation} \xrightarrow{K_1} V+I, \qquad (\text{A}\cdot 1)$$

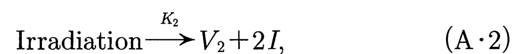

$$\text{Irradiation} \xrightarrow{K_2} V_2+2I, \qquad (\text{A}\cdot 2)$$

$$V+I \xrightarrow{K_{IV}} \text{Null}, \qquad (\text{A}\cdot 3)$$

$$V \xrightarrow{K_{VS}} \text{sinks}, \qquad (\text{A}\cdot 4)$$

Table A·I. Rate equations, definitions of reaction constants and input parameters used in the calculation.

Rate equations:

$$\frac{\mathrm{d}[V]}{\mathrm{d}t}=K_1-K_{IV}[I][V]-K_{VS}[V]-2K_{V_2}[V]^2-K_{VP}[V]([P_0]-[VP])+K_{IV_2}[I][V_2]$$

$$\frac{\mathrm{d}[I]}{\mathrm{d}t}=K_1+2K_2-K_{IV}[I][V]-K_{IS}[I]-K_{IV_2}[I][V_2]-K_{IVP}[I]/[VP]$$

$$\frac{\mathrm{d}[V_2]}{\mathrm{d}t}=K_2+K_{V_2}[V]^2-K_{IV_2}[I][V_2]$$

$$\frac{\mathrm{d}[VP]}{\mathrm{d}t}=K_{VP}[V]([P_0]-[VP])-K_{IVP}[I][VP]$$

Reaction constant:

$K_1=\eta_V\cdot i$, $K_2=\eta_{V_2}\cdot i$, $K_{VS}=\alpha D_V$, $K_{IS}=\alpha D_I$, $\alpha=\pi^2(1/A^2+1/B^2+1/C^2)$

$K_{IV}=4\pi R(D_I+D_V)$, $K_{IV_2}=K_{IVP}=4\pi RD_I$, $K_{V_2}=8\pi RD_V$, $K_{VP}=4\pi RD_V$

Parameter	Value
Production rates:	$\eta_V=10$ cm^{-1}, $\eta_{V_2}=0.03$ cm^{-1}
Beam current:	$i=10$ μA
Capture radius:	$R=5$ Å
Diffusion coefficients:	$D_V=4\times 10^{-9}$ cm^2/s, $D_I=3\times 10^{-5}$ cm^2/s
Size of crystal:	$A=B=0.5$ cm, $C=1$ cm
Initial phosphorus concentration:	$[P_0]=2\times 10^{16}$ cm^{-3}

$$I \xrightarrow{K_{IS}} \text{sinks}, \tag{A·5}$$

$$V+V \xrightarrow{K_{V_2}} V_2, \tag{A·6}$$

$$V+P \xrightarrow{K_{VP}} VP, \tag{A·7}$$

$$V_2+I \xrightarrow{K_{IV_2}} V, \tag{A·8}$$

$$VP+I \xrightarrow{K_{IVP}} P. \tag{A·9}$$

Equations (A·1) and (A·2) show the direct formation of a monovacancy (V), a single interstitial (I) and a divacancy (V_2) upon irradiation. Equation (A·3) shows the recombination of a monovacancy and a single interstitial. Equations (A·4) and (A·5) show the annihilation of a monovacancy and a single interstitial at their sinks. Equations (A·6) and (A·7) show the formation of a divacancy or a VP pair through the combination of two monovacancies or by combination of a monovacancy and an isolated phosphorus atom. Equations (A·8) and (A·9) show the annihilation of a divacancy and a VP pair due to the recombination with a single interstitial. K_i denotes the reaction constant.

Thus, we set up the chemical rate equations shown in Table A·I. The brackets [ ] denote the concentration. In the case of phosphorus-free (undoped) Si, we neglect the terms related to VP pairs. This is the case for Si:B specimens.[38] The reaction constants are also defined in the table. The specimen is assumed to be the rectangular with the size of A×B×C. Sinks are assumed to be on the surface of the specimen. The fluence is given by $i \cdot t$. Since it seems to be difficult to solve these rate equations in analytical forms, we solved them numerically using the input parameters shown in Table A·I. The production rates of monovacancies and divacancies with 15 MeV electron irradiation were cited from refs. 46 and 1, respectively. The diffusion constants of monovacancies and single interstitials were cited from ref. 47. The capture radii are assumed to be 5 Å in all cases. This is thought to be an effective interaction radius for elastic interaction among neutral defects.[48]

Figure A·1 shows the result of numerical calculations. The concentration of divacancies in undoped Si increases linearly with the fluence. This agrees with the experimental result for Si:B specimens shown in Fig. 4. From Fig. A·1, the linear dependence of the concentration of divacancies may be interpreted in terms of the concentrations of monovacancies and interstitials rapidly reaching the stationary values in the low fluence range. On the other hand, the concentration of divacancies in phosphorus-doped Si is rather low in the low fluence range and increases rapidly in the high fluence range. The concentration of VP pairs increases with fluence and tends to saturate in the high fluence range. These behaviors are similar to the experimental results for Si:P specimens shown in Fig. 4. It is also noted that the behaviors of concentrations of monovacancies and single interstitials are different from those in undoped Si. Namely, the concentrations of monovacancies or single interstitials are somewhat lower or higher

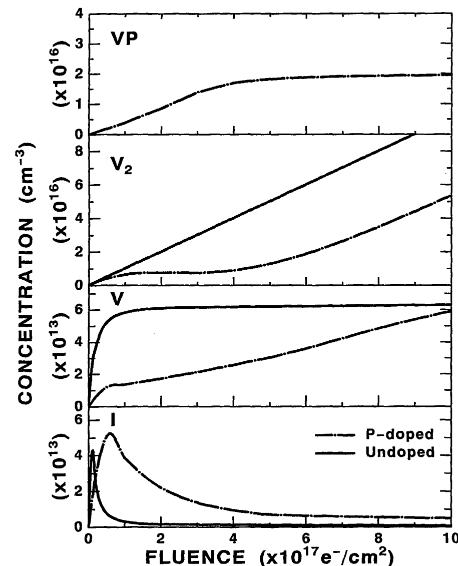

Fig. A·1. The concentrations of VP pairs (VP), divacancies (V_2), monovacancies (V) and single interstitials (I) as a function of fluence. Solid lines are for undoped Si. Chained lines are for phosphorus-doped Si.

than those of undoped Si and tend to approach stationary values in the high fluence range. The nonlinear fluence dependence of the concentration of divacancies in phosphorus doped Si may be interpreted in the following way. In the lower fluence range, monovacancies generated by irradiation are trapped by phosphorus atoms to form VP pairs. This results in the reduction of free monovacancies and yields excess interstitials. As a result, the formation rate of divacancies due to the pairing of monovacancies is reduced and recombinations between divacancies and single interstitials are enhanced; hence the concentration of divacancies is suppressed. With high fluence, the concentration of VP pairs approaches the saturated value, namely VP pairs are no longer produced. This results in the increase of free monovacancies and reduction of excess interstitials due to the mutual recombinations. As a result, the concentration of divacancies increases rapidly.

As mentioned in §3.1, Svensson and co-workers[15,17] also found a similar nonlinear fluence dependence of the concentration of divacancies in tin-doped Si. They explained it in terms of the trapping of monovacancies, but did not consider the behavior of single interstitials. Our results show that the linear and nonlinear fluence dependences of the concentration of divacancies may be fully interpreted by taking into account both the trapping of monovacancies by phosphorus atoms and the behaviors of interstitials.

1) J. W. Corbett: *Solid State Physics*, eds. F. Seitz and and D. Turnbull (Academic Press, New York and London, 1966) Suppl. 7, Chap. 3, p. 59.
2) G. D. Watkins, J. R. Troxell and A. P. Chatterjee: *Deep Centers in Semiconductors*, ed. S. T. Pantelides (Gordon and Breach Science Publishers, New York, 1986) Chap. 3, p. 147.
3) G. D. Watkins: Inst. Phys. Conf. Ser. **46** (1978) 16.
4) G. D. Watkins and J. W. Corbett: Phys. Rev. **138** (1965) 543.

5) L. J. Cheng, J. C. Corelli, J. W. Corbett and G. D. Watkins: Phys. Rev. **152** (1966) 761.
6) M. T. Lappo and V. D. Tkachev: Sov. Phys.-Semicond. **4** (1971) 1882.
7) J. Svensson, B. G. Svensson and B. Monemer: Mater. Sci. Forum **38–41** (1989) 451.
8) H. Y. Fan and A. K. Ramdas: J. Appl. Phys. **30** (1959) 1127.
9) F. C. Merlet, B. Pajot, D. T. Don, C. Porte, B. Clerjaud and P. M. Mooney: J. Phys. C: Solid State Phys. **15** (1982) 2239.
10) A. H. Kalma and J. C. Corelli: Phys. Rev. **173** (1968) 734.
11) R. C. Young and J. C. Corelli: Phys. Rev. B **5** (1972) 1455.
12) A. O. Evwaraya and E. Sun: J. Appl. Phys. **47** (1976) 3776.
13) S. D. Brotherton and P. Bradly: J. Appl. Phys. **53** (1982) 5720.
14) B. G. Svensson, B. Mohadjeri, A. Hallen, J. H. Svensson and J. W. Corbett: Phys. Rev. B **43** (1991) 2292.
15) B. G. Svensson, J. Svensson, J. L. Lindström, G. Davies and J. W. Corbett: Appl. Phys. Lett. **51** (1987) 2257.
16) B. G. Svennson and M. Willander: J. Appl. Phys. **62** (1987) 2758.
17) B. G. Svensson and J. L. Lindström: J. Appl. Phys. **72** (1992) 5616.
18) G. A. Samara: Phys. Rev. B **39** (1989) 12764.
19) G. D. Watkins and J. W. Corbett: Phys. Rev. **134** (1964) 1359.
20) H. Saito and M. Hirata: Jpn. J. Appl. Phys. **2** (1963) 678.
21) M. Hirata, M. Hirata and H. Saito: J. Phys. Soc. Jpn. **27** (1969) 405.
22) L. C. Kimerling, H. M. DeAngelis and J. W. Diebold: Solid State Commun. **16** (1975) 171.
23) *Positron Solid-State Physics*, eds. W. Brandt and A. Dupasquier, (North Holland, Amsterdam, 1983).
24) For example, M. J. Puska and R. M. Nieminen: Rev. Mod. Phys. **66** (1994) 841.
25) For example, P. A. Kumar, K. G. Lynn and D. O. Welch: J. Appl. Phys. **76** (1994) 4935.
26) P. Mascher, S. Dannefaer and D. Kerr: Phys. Rev. B **40** (1989) 11764.
27) M. Shimotomai, Y. Ohgino, H. Fukushima, Y. Nagayasu, T. Mihara, K. Inoue and M. Doyama: Inst. Phys. Conf. Ser. **59** (1981) 241.
28) M. Kwete, D. Segers, M. Drikens, L. D. Vanpraet and P. Clauws: Appl. Phys. A **49** (1989) 659.
29) J. Mäkinen, P. Hautojärvi and C. Corbel: J. Phys. Condensed Matter **4** (1992) 5173.
30) For example, K. Seeger: *Semiconductor Physics* (Springer-Verlag, Berlin, 1982) 2nd ed., Chap. 4, p. 61.
31) P. Kirkegaard, N. J. Pederson and M. Eldrup: PATFIT-88, Riso-M-2704 (1989).
32) J. S. Blakemore: *Semiconductor Statistics* (Dover Publications, New York, 1987) Chap. 3, p. 164.
33) H. Ono and K. Sumino: J. Appl. Phys. **57** (1985) 287.
34) A. Kawasuso, M. Suezawa and K. Sumino: Unpublished.
35) J. A. Van Vechten: *Handbook of Semiconductors*, eds. T. S. Moss and S. P. Keller (North Holland, Amsterdam, 1980) Vol. 3, Chap. 1, p. 14.
36) H. Kamiyama: Ph. D. Thesis, Tohoku University, Sendai, Japan, 1989.
37) A. C. Damask and G. J. Dienes: *Point Defect in Metals* (Gordon and Breach, New York, 1963).
38) Undoped Si means that no vacancy-impurity pairs are formed. Since the vacancy-boron pairs rarely survive at room temperature, the boron-doped Si could be regarded as undoped Si.
39) J. Mäkinen, C. Corbel, P. Hautojärvi, P. Moser and F. Pierre: Phys. Rev. B **39** (1989) 10162.
40) A. Kawasuso, M. Hasegawa, M. Suezawa, S. Yamaguchi and K. Sumino: unpublished.
41) M. Kwete, D. Segers, M. Drikens, L. D. Vanprate and P. Clauws: Phys. Status Solidi a **122** (1990) 129.
42) A. Kawasuso, M. Hasegawa, M. Suezawa, S. Yamaguchi and K. Sumino: to be published in Mater. Sci. Forum.
43) S. Mäkinen and M. J. Puska: Phys. Rev. B **40** (1989) 12523.
44) A. Kawasuso, M. Hasegawa, M. Suezawa, S. Yamaguchi and K. Sumino: Hyperfine Interactions **84** (1994) 397.
45) M. J. Puska, C. Corbel and R. M. Nieminen: Phys. Rev. B **41** (1990) 9980.
46) O. S. Oen: ORNL-4897, Oak Ridge National Laboratory, Oak Ridge, Tennessee, The United States of America, 1973.
47) G. S. Oehrlein, I. Krafcsik, J. L. Lindström, A. E. Jaworowski and J. W. Corbett: J. Appl. Phys. **54** (1983) 179.
48) J. W. Corbett, J. C. Bourgoin, L. J. Cheng, J. C. Corelli, Y. H. Lee, P. M. Mooney and C. Weigel: Inst. Phys. Conf. Ser. **31** (1977) 1.